

**THE PENNSYLVANIA STATE UNIVERSITY
SCHREYER HONORS COLLEGE**

DEPARTMENT OF BIOLOGY

**THE FUNCTION OF MICROTUBULE POLARITY IN DROSOPHILA
DENDRITES**

**MANPREET KAUR PARMAR
SPRING 2012**

A thesis
submitted in partial fulfillment
of the requirements
for a baccalaureate degree
in Biology
with honors in Biology

Reviewed and approved* by the following:

Melissa Rolls
Assistant Professor of Biochemistry and Molecular Biology
Thesis Supervisor

Stephen Schaeffer
Professor of Biology
Honors Adviser

Gong Chen
Associate Professor of Biology
Faculty Reader

Douglas Cavener
Professor and Head of Biology

* Signatures are on file in the Schreyer Honors College.

Abstract

The nervous system is composed of billions of neurons that communicate rapidly via electrical and chemical signaling to receive, transmit, and integrate information flow throughout the body. Within each neuron, microtubules serve as tracks for long-range transport that is essential for maintaining the cell's function and survival. The purpose of this research project was to understand how polarity of dendrite microtubules contributes to polarized trafficking of proteins and organelles in a neuron. Since *Drosophila melanogaster* share many neuronal properties with vertebrates, these fruit flies served as a useful model system for studying neuronal cell biology. Three assays were completed to determine the effect of altering the minus-end-out microtubule orientation of ddaE dendrites to evenly mixed. In all cases, Kap3RNAi was utilized to create an experimental group consisting of larvae with an evenly mixed microtubule orientation, and rtnl2RNAi was used to establish a control group of larvae with predominately minus-end-out microtubules in their dendrites. The class I neuron was imaged with confocal microscopy and analyzed using Image J. Results showed that altering microtubule polarity did not change dendrite morphology significantly but did affect aspects of endosome movement and mitochondrial distribution strongly. A deeper understanding of the contribution of microtubule polarity to polarized trafficking of organelles in the dendrites may aid in advancing research about the structural and functional specialization of dendrites as well as medical therapies for neurodegenerative diseases.

Acknowledgements

I thank Dr. Melissa Rolls for giving me the unique opportunity to research in her lab. Her support gave me the chance to work with cutting-edge technology in the field of molecular biology, explore neural research, and grow as a student. With Dr. Rolls' guidance and motivation, I enhanced my research, critical thinking, communication, and teamwork skills, and her genuine enthusiasm for neural research fueled my passion to learn about neuroscience and genetics. I also want to thank the following graduate students for serving as mentors and teaching me numerous experimental procedures about manipulating genetics, live-imaging with confocal microscopy, culturing fruit flies, and data analysis: Michelle Stone, Floyd Mattie, Michelle Nyguen, Megan Stackpole, Juan Tao, Li Chen, and Melissa Long. Furthermore, I want to show my gratitude to NASA for awarding me the Women in Science and Engineering scholarship as well the Schreyer Honors College for providing me the Summer Research grant, both of which aided in funding my project. Finally, I want to thank Dr. Rolls, Dr. Stephen Schaeffer, Dr. Gong Chen, and Dr. Douglas Cavener for evaluating my undergraduate honors thesis.

Table of Contents

Introduction.....	1
Neuron.....	1
Microtubule Polarity.....	2
Project Synopsis.....	4
Directed Microtubule Growth.....	5
Drosophila melanogaster as a Model System.....	6
Significance of Project	8
Materials & Methods.....	10
Fly Stocks.....	10
Live Imaging of da Neurons.....	11
Analysis of EB1-GFP and Rab4-RFP Dynamics.....	11
Statistical Analysis.....	13
Results.....	15
Altering microtubule polarity does not affect dendrite morphology.....	15
Microtubule polarity affects the abundance of mobile endosomes and the direction of endosome trafficking.....	20
Microtubule polarity does not influence overall mitochondrial distribution, but affects branch point occupancy.....	27
Discussion.....	34
References	40

Introduction

Neuron

Whether it is the aroma of perfume or the chimes of the Old Main clock, the nervous system is responsible for processing stimuli from the environment and sending information over long distances in the human body. A neuron is the basic unit of the nervous tissue (Campbell *et al.*, 2008).

Neurons are highly compartmentalized in morphology and function (Stone *et al.*, 2008). This neuronal differentiation is controlled by a series of proteins such as kinases, phosphatases, small GTPases, and scaffolding proteins; it can result from the addition of insulin-like growth factor 1 and the lack of cell-to-cell contact or extracellular matrix molecules (Conde *et al.*, 2009). For a vertebrate neuron, cell bodies can be found in the brain, spinal cord, and peripheral ganglia. Most of the proteins are synthesized in the cell bodies. Dendrites synapse with axons in order to receive signals and transmit them towards the cell body for processing. Alternatively, axons carry signals away from the soma and towards other neurons or output cells (Campbell *et al.*, 2008). Vertebrate axons have fewer ribosomes and no Golgi outposts compared to dendrites (Craig *et al.*, 1994). Moreover, while the single processes of axons usually divide into branches at synapses, dendrites are more extensively branched throughout their structure to cover a larger surface area (Campbell *et al.*, 2008).

Microtubule Polarity

A major task of the neuron is to transfer proteins and membranes from the cell body to distant regions in axons and dendrites. This intracellular transport is essential to maintain the cell's function and survival, and the tracks for this long-range directional transport consist of microtubules (Black *et al.*, 1989), cylindrical structures of alpha and beta tubulin heterodimers. Neurons have polarized microtubules throughout their processes that can be categorized into two groups: minus-end-out and plus-end-out microtubules. Minus-ends of these microtubules usually have noncentrosomal microtubule arrangements (Bartolini *et al.*, 2006), while plus-ends interact with several proteins and are involved with assembly and disassembly. This microtubule polarity directs traffic in the cytoplasm, and thus, it establishes an asymmetric distribution of different organelles. Molecular motor proteins transport microtubules into axons and dendrites and dictate the microtubule polarity orientation. Different groups of microtubule-binding proteins and membrane proteins are found in axons and dendrites (Baas *et al.*, 2010). Cytoplasmic dynein is a motor that transports vesicles towards the minus ends of microtubules, whereas kinesin proteins are plus-end directed motors (Lodish *et al.* 2000).

Microtubule orientation is distinctly different in axons and dendrites (Rolls *et al.*, 2007). Studies have found that microtubules in vertebrate dendrites have mixed orientation, while axons have all plus-ends distal to the cell body. Experiments involving the hook labeling method have shown an equal number of plus-end-out and minus-end-out microtubules throughout the dendrites of frog mitral cells (Burton 1988). In this hook decoration method, microtubules are incubated with tubulin and a buffer that stimulates

polymerization, resulting in tubulin protofilament hooks on the walls of the microtubules. Electron micrographs are then used to determine the handedness of the hooks, which denotes the microtubule orientation. When one's fingers are curved in the direction of the hooks, the thumb points towards the minus-end of the microtubule (Kuo 2007). Similarly, mixed microtubule orientation was evident in proximal dendrites of cultured rodent interneurons via both the hook method and assays involving microtubule plus-end binding protein, EB3- green fluorescent protein (GFP) (Stepanova *et al.*, 2003). In hippocampal neurons, the presence of minus-end-out microtubules initiates dendritic specialization and growth (Baas *et al.* 2011).

Unlike previous studies involving the cultured vertebrate neurons, live imaging experiments have found that in *Drosophila*, the dendrite is defined by microtubules with minus-ends distal to the cell body (Stone *et al.*, 2008). End-binding protein 1 (EB1) is a commonly used plus-end tracking protein, or +TIP, that localizes specifically to growing microtubule plus ends (Lansbergen, *et al.*, 2006). Using stable cell lines expressing EB1-GFP, the directional movement of these fluorescent comets was tracked with confocal microscopy and quantified. In *Drosophila* sensory neurons, assays using EB1-GFP dynamics have shown that more than 95% of microtubules in dendrites of highly branched dendritic arborization (da) neurons have minus-ends distal to the soma (Rolls *et al.*, 2007). Moreover, experiments involving EB1-GFP have shown that minus-end-out microtubules are predominant not only in *Drosophila* sensory neurons but also in interneurons and motor neurons, making them the “conserved signature” of *Drosophila* dendrites; the predominance of minus-end-out microtubules in these proximal dendrites ranged from 88% to 94% (Stone *et al.*, 2008). EB1-GFP dynamics have further shown

that microtubules growing around dendritic branch points turn toward the cell body along stable plus-end-out microtubules 98% of the time (Mattie *et al.*, 2010). Recent studies involving injury trauma and neuronal regeneration have also provided support for this “signature minus-end-out” microtubule orientation in dendrites by demonstrating that polarized *Drosophila* dendrites can convert into axons after complete reversal of microtubule polarity (Rolls *et al.*, 2009).

Project Synopsis

Neuronal polarity refers to the differences between axons and dendrites. Past research suggests that microtubule polarity of axons and dendrites may contribute to neuronal polarity. For example, organelles traveling along microtubules toward plus-ends can be found in axons and dendrites, but organelles moving toward minus-ends of microtubules have only been seen in dendrites (Baas, *et al.* 2011). Also, dendrites have proteins and organelles that are relatively scarce in axons, such as the rough endoplasmic reticulum, the Golgi apparatus, and neurotransmitter receptors (Craig *et al.*, 1994).

The purpose of this research was to understand how microtubule polarity contributes to polarized trafficking of proteins in dendrites and, thus, their specialization in structure and function. Does changing microtubule orientation alter dendritic morphology or disrupt organelle trafficking and distribution within the dendrite? To meet this goal, tagged markers were used to examine how different characteristics of *Drosophila melanogaster* dendrites are affected when microtubule orientation is changed from minus-end-out to about evenly mixed. Using data collected from confocal microscopy, both qualitative and quantitative analyses were carried out with Image J program. It was hypothesized altering dendritic microtubule orientation from minus-end-

out to evenly mixed would disrupt organelle transport and distribution.

Drosophila melanogaster as a Model System

Drosophila melanogaster is a valuable model system for research in neuroscience. Fruit flies have a short life cycle, allowing several experiments to be run in a give time span. Their transparent larval bodies make their neuronal processes easily observable via microscopy, and they can be maintained with little difficulty at a low cost. Using the abundance of genetic tools, researchers can manipulate gene expression in *Drosophila* and observe the effects on neurons *in vivo*. Many proteins, such as EB1, are similar between fruit flies and vertebrates (Rogers *et al.*, 2002), which allows observations and conclusions from research with *Drosophila* to be applied to vertebrates, especially humans. Furthermore, the major types of intracellular compartmentalization are also conserved between *Drosophila* and vertebrates; like axons and dendrites of vertebrate neurons, those of *Drosophila* differ in both microtubule binding proteins and filament orientation (Rolls *et al.*, 2007). Therefore, *Drosophila* is an important model system that can be easily manipulated to study neuronal organization on a molecular level.

In *Drosophila*, dendritic arrangement is relativity simple and uniformly polarized with predominantly minus-end-out microtubules (Stone *et al.*, 2008). Therefore, transport specifically in dendrites can be studied by targeting these microtubules. In particular, the *Drosophila* dendritic arborization (da) neurons, which are sensory neurons found extensively on the body wall of *Drosophila* larvae, are easily studied due to their unique dendritic morphologies (Anderson *et al.*, 2005). The four different subclasses of dendritic aborization (da) neurons vary in their pattern of dendritic branching (Grueber *et al.*,

2002). In class II to IV, growing microtubules turn at a smaller angle toward the cell body than away from the soma, and so growth towards the cell body is favored. However, the class I neuron has a comb-like structure, and its branch angles are closer to right angles and similar for both the inward and outward turns. Compared to the class II-IV neurons, the comb dendrite of the class I neuron has a larger average inward turn angle and a smaller average outward turn angle. Since directed microtubule growth at branch points plays an important role in establishing microtubule polarity, the class I dorsal dendritic arborization neuron E (ddaE) experiences the strongest polarity defects when kinesin-2 motor levels are reduced by RNAi (Mattie *et al.*, 2010). Consequently, the assays in this project were focused on the ddaE class I neuron.

Directed Microtubule Growth

Growing microtubules have two potential avenues. A microtubule plus-end extending from a distal dendrite through a branch point into another distal dendrite forms a plus-end-out microtubule in the latter dendrite. However, assays of EB1-GFP dynamics in da neurons have shown that this orientation only had a 2% prevalence, while the minus-end-out microtubule signature of the *Drosophila* dendrite had a 98% prevalence. Thus, dendritic microtubules primarily grow towards the cell body at dendritic branch points (Mattie *et al.*, 2010).

Live imaging experiments have shown that the following three requirements are necessary for establishing this uniform microtubule polarity in dendrites: directed microtubule growth, +TIPs, and the kinesin-2 motor. Using EB1-GFP dynamics, the growing plus ends of microtubules were tracked in dorsal clusters of da neurons. Results from two-color live imaging of *Drosophila* larvae expressing tau-GFP and EB1-GFP

showed that plus ends of growing microtubules track stable existing microtubules in dendrites and move towards their plus ends (Mattie *et al.*, 2010).

Kinesins are proteins that walk toward the plus-ends of microtubules. Kinesin-2 (KIF3) is a heterotrimeric protein with two motor subunits, Klp64D and Klp68D in *Drosophila*, and a globular, accessory subunit called Kap3 (Mattie *et al.*, 2010). In mammalian cells, Kap3 interacts with the microtubule plus-end binding protein (+TIP) adenomatous polyposis coli (Jimbo, *et al.*, 2002). After reducing the levels of any of the three subunits of the kinesin-2 motor using RNA interference (RNAi), results from scoring the EB1-GFP comets showed an increase in the number of plus-end-out microtubules to 20% to 28%. More specifically, Kap3RNAi showed an increase to approximately 24% of plus-end-out microtubules, while Klp68DRNAi and Klp64DRNAi showed an increase to 20% and 28% respectively. Without kinesin-2, the undirected microtubule growth prevented the formation of the uniform minus-end-out microtubule polarity in dendrites, and in this way, the microtubule polarity became disorganized (Mattie *et al.*, 2010). Therefore, in this project, to alter the microtubule orientation of dendrites from minus-end-out to evenly mixed, RNAi was used to reduce the levels of the kinesin-2 motor.

Moreover, upon decreasing the kinesin-2 subunits using RNAi, more plus-end-out microtubules were present in the comb dendrite than the other da neurons. As described previously, the pattern of the dendrite branch angles in the comb dendrite is responsible for this stronger phenotype in the class I neuron, compared to the other da neuron classes, upon reduction of the kinesin-2 levels (Mattie *et al.*, 2010). Therefore, this project focused on analyzing effects in the class I neuron ddaE.

Lastly, when EB1 levels were reduced using RNAi, the number of dendrite-to-dendrite microtubule tracks visible with Rab4-RFP using confocal microscopy doubled, representing an increased number of dendrites with mixed polarity (Mattie *et al.*, 2010). Consequently, EB1 is necessary to maintain uniform dendritic microtubule polarity, and in this project, the fruit fly lines used to examine dendrite morphology included EB1 expression.

Significance of Project

The integrity of intracellular transport via microtubules is essential for the function and survival of neurons. Consequently, alterations to this directed transport can cause defects in the neurons and lead to neurodegenerative diseases. While other cells in the body may be replaceable, most neurons must last an entire lifetime (Campbell *et al.*, 2008). A deeper understanding of neuronal polarity and microtubule polarization may help shed light to the basic processes that cause these diseases and aid in designing drug therapies for nerve injury repair and regeneration. For example, the da neurons in mammals, which are usually located in the midbrain, are involved in motor control, neuroendocrine hormone release, cognition and emotion, reward, and psychiatric and neurological disorders (Perrone-Capano *et al.*, 2000). Examining similar neurons in *Drosophila*, as was done in this research project, may help understand the physiology of the nervous system and advance neurological medicine. Although this research is relevant to the field of health sciences, the work is also important to answer existing questions about the relationship between dendritic transport and microtubule polarity and also bring forth novel research questions for study. Thus, purpose of this research was to understand how microtubule polarity contributes to polarized trafficking of proteins in dendrites and,

thus, their specialization in structure and function.

Materials & Methods

Fly Stocks

All the fly lines were kept at 25°C. For the dendrite morphology assay, progeny were collected from the crosses of *dicer2*; 221 EB1-GFP/TM6 with VDRC 45400 *Kap3RNAi* and VDRC 33320 *Rtnl2rna*. Virgin female flies of *Kap3RNAi* and *Rtnl2rna* were collected after incubating the fly lines for a maximum of 6 hours at room temperature or 12 hours at 18°C. The females from each RNAi line were crossed with males from *dicer2*; 221EB1/TM6. Every 24 hours, the food cap with the larvae was collected in Petri dishes and allowed to mature for 72 hours at 25°C. Using the UAS-Gal4 binary expression system, GFP-tagged microtubule binding proteins were expressed in the *Drosophila* neurons. The *elav* (embryonic lethal, abnormal vision)-Gal4 driver was used to activate gene transcription of EB1-GFP, proteins that bind to growing microtubule plus-tips and are visible as green comets; the greatest green fluorescence is found at the plus-ends. RNAi was used to knock down *Kap3* in the mutant fly neurons and alter microtubule orientation, and the UAS-Dicer2 transgene was added to increase the effectiveness of the RNAi in the *Drosophila* neurons (Dietzl *et al.*, 2007).

For the endosome trafficking assay, the same cross procedure was used to prepare the progeny, as in the previous experiment. Virgin female *Drosophila melanogaster* of VDRC 33320 *Rtnl2rna* and VDRC 45400 *Kap3RNAi* were each crossed with males of the upstream activation sequence (UAS)-Rab4-RFP; *elav*-Gal4, UAS-Dicer2. The Rab4/RFP is a membrane trafficking protein that localizes to endosomes and fluoresces red (Rolls *et al.*, 2010). Likewise, for the mitochondria assay, virgin females of VDRC 33320 *Rtnl2rna* and VDRC 45400 *Kap3RNAi* were crossed with males from *Dicer2*,

mCD8RFP/cyo; elav-Gal4, mitoGFP. Driven by elav, mito-GFP was used to label the mitochondria, and mCD8-red fluorescent protein (RFP), a protein that localizes on the plasma membrane, was used to outline the structure of the dendrites.

To prepare for a future Golgi localization assay in dendrites involving the fly line 477, mCD8-RFP; dicer2, GalT-YFP, virgin female UAS-mCD8-RFP, 477Gal4 fruit flies were crossed with UAS-GalT-YFP, UAS-dicer2 males. A recombination scheme was also begun to create fly line with Rab-3, which is involved with synaptic transmission and neurotransmitter release, and another line with ANF-GFP (UAS-ANF-EMD, 221 Gal4/TM6 line) to study effects of altering microtubule orientation on the distribution of the atrial natriuretic factor in dendrites.

Live Imaging of da Neurons

Live, three-day old larvae were cleaned in Schneider's solution and mounted on agarose-padded slides with their dorsal side up. After a cover slip was placed gently on top of the larvae and secured in place with scotch tape, the larvae were imaged with the confocal microscope Zeiss LSM510 or Olympus FV1000. Several consecutive live images of the class I neuron, primarily in the 3rd and 4th hemisegments from the mouth, were taken. One image was taken each second, and only a single class I neuron was imaged in each larvae. The 40X objective was used on the Olympus, and the 60X objective was used on the Zeiss.

Analysis of EB1-GFP and Rab4-RFP Dynamics

Using an image-processing program called Image J, Z-stacks were compiled from the time series videos obtained with confocal microscopy, and different properties of the class I neuron were evaluated qualitatively and quantitatively to determine the differences

between the control and experimental groups. In the morphology assay, dendrite length beginning from the junction at the cell body and extending to the last branch point of the primary dendrite was measured in pixels/um with Image J tools.

For the endosome trafficking assay, moving comets in the primary dendrite that were clearly visible in at least three consecutive frames with “gray scale” settings in Image J were tracked and counted manually. As depicted in figure 1, each endosome moving toward the soma was labeled “To Soma,” and each endosome moving away was tagged “Away Soma.” If an endosome changed direction midway in its transport, each movement was counted. For example, if the comet initially moved towards the soma and then turned around to move away from the cell body, the movement would be counted as both “To Soma” and “Away Soma.” Also, if an endosome moved for a certain time in one direction, stopped, and then continued moving in that direction, the movement was counted twice in the same direction.

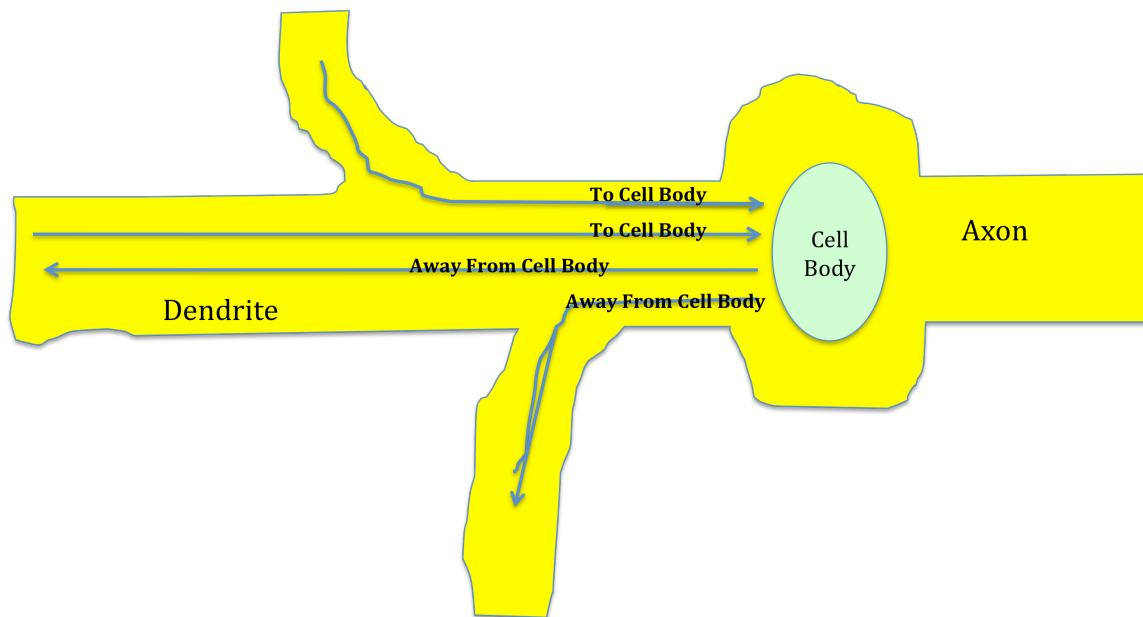


Figure 1: Dendrite Scoring Rubric

This figure represents a model for the quantification of endosome trafficking in the primary dendrite of the class I neuron. Only dark and distinct dots were counted. Continuous movements in one

direction were counted once as either “To Soma” or “Away Soma.” Motions, during which the direction changed, were tallied for each direction, and discontinuous motions in the same direction were counted multiple times for that direction accordingly. In this way, each movement was accounted.

In the mitochondrial distribution assay, mitoGFP comets were counted manually. For each larva imaged, the total number of mitochondria in the primary dendrite and each of the secondary branches were counted and summed. In addition, using the tracing tools in Image J, the lengths of the primary dendrite and each of the secondary dendrites were measured in pixels/um and added. All the length values were scaled to lengths in micrometers for a 40X objective and a 0.7x zoom. Dividing the number of mitochondria by the summed lengths of the primary and secondary dendrite branches gave the number of mitochondria per unit length in micrometers. Furthermore, the number of branch points with localized mitochondria clusters and the number of mitochondria at each branch point were also scored; a parameter of three microns from each branch point was used as a standard. The numbers of mitochondria at each of the branch points were averaged in each sample, and these values were then averaged for both the control and experimental groups to get a mean number of mitochondria per branch point for each group. Likewise, the number of occupied branch points for each individual sample was found, and then these values were averaged to estimate the mean branch point occupancy.

Finally, in each assay, the results for the control and experimental groups were compared quantitatively and qualitatively, and the percent difference was calculated.

Statistical Analysis

For each set of data points, the overall mean, variance, standard deviation, and standard error were found. The overall mean was found by summing each of the individual values and then dividing by the total number of data points in each group.

Next, each individual data point was subtracted by this mean, and the differences were squared individually. Variance was found by dividing the sum of these differences by one

less than the sample size, as shown by the following formula: $\frac{\sum (x_1 - \bar{x})^2}{n - 1}$. “n” is the

number of data points, and \bar{x} is the overall mean. Standard deviation was found by taking the square root of the variance, and the standard error was calculated by dividing the standard deviation by the square root of the sample size.

Next, a two-tailed t-test was performed to determine whether the difference between the control and experimental groups was significant. The observed t-value was

calculated using the following formula: $\frac{|\bar{x}_1 - \bar{x}_2|}{\sqrt{\frac{(n_1 - 1)s_1^2 + (n_2 - 1)s_2^2}{df}} * \sqrt{\frac{n_1 + n_2}{n_1 n_2}}}$. “s” is the

standard deviation, and “df” is the degrees of freedom ($n_1 + n_2 - 2$).

When reading the chart of critical t-values, the alpha level was set to 0.05. If the observed t-value was less the critical t-value, the null hypothesis was accepted, and it was concluded that no significant difference existed between the two mean values. However, if the observed t-value was greater than or equal to the critical t-value, the null hypothesis was rejected, and it was concluded that there was a significant difference between the two mean values.

Results

Altering microtubule polarity does not affect dendrite morphology

The goal of the first assay was to determine the effect of disrupting minus-end-out microtubule orientation on dendritic morphology. It was hypothesized that the growth pattern and resulting morphology of the dendrite would change upon altering the microtubule orientation. The experimental group consisted of Kap3RNAi larvae with an evenly mixed microtubule orientation. The RNAi knockdown increased the percentage of plus-end-out microtubules in dendrites, resulting in the minus-end out microtubule signature orientation of dendrites to change to evenly mixed. The control group had dendrites with a minus-end-out microtubule orientation; RNAi was used to reduce the levels of reticulon 2 (*rtnl2*), which is a membrane protein associated with the endoplasmic reticulum. This protein is usually 200-1200 amino acids in length, and its genes are found in a wide range of eukaryotes, fungi, plants, and animals (Oertle *et al.*, 2003). No phenotype is observed when *rtnl2* in fruit flies is knocked down by RNAi (Mattie *et al.*, 2010).

Contrary to the hypothesis, the results did not show a notable qualitative difference between the control and experimental groups. A sample size of 10 fruit fly larval neurons was used for both the experimental group and the control group. Overall, the comb-like shape of the neuron remained consistent. As shown in figures 2 and 3, the class I neurons in both groups had dendrites that extended outwards to form a “C” shape. Relative to the other neurons in the dorsal cluster, the class I neuron was spaced farther away and had a shorter primary dendritic branch and fewer secondary offshoots.

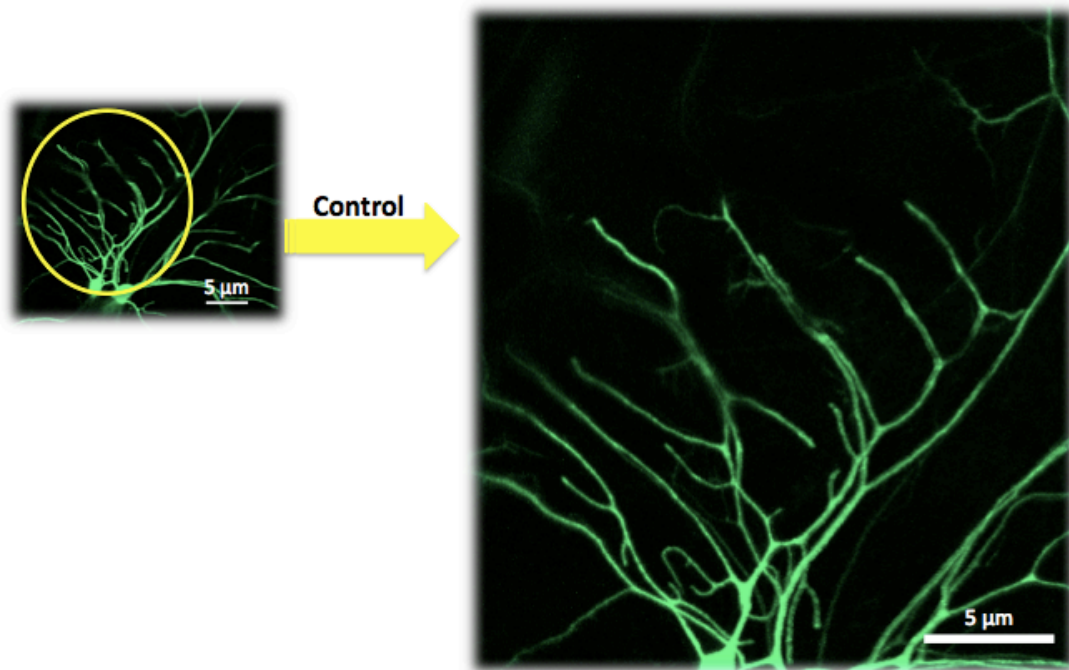


Figure 2: Dendrite Morphology of Control ddaE

This image was obtained from live imaging with confocal microscopy. It represents the class I neuron's dendrites in a three-day old larvae from the control group. The green fluorescence is due to the expression of EB1-GFP in the larvae. The ddaE is distinguished by its comb dendrite.

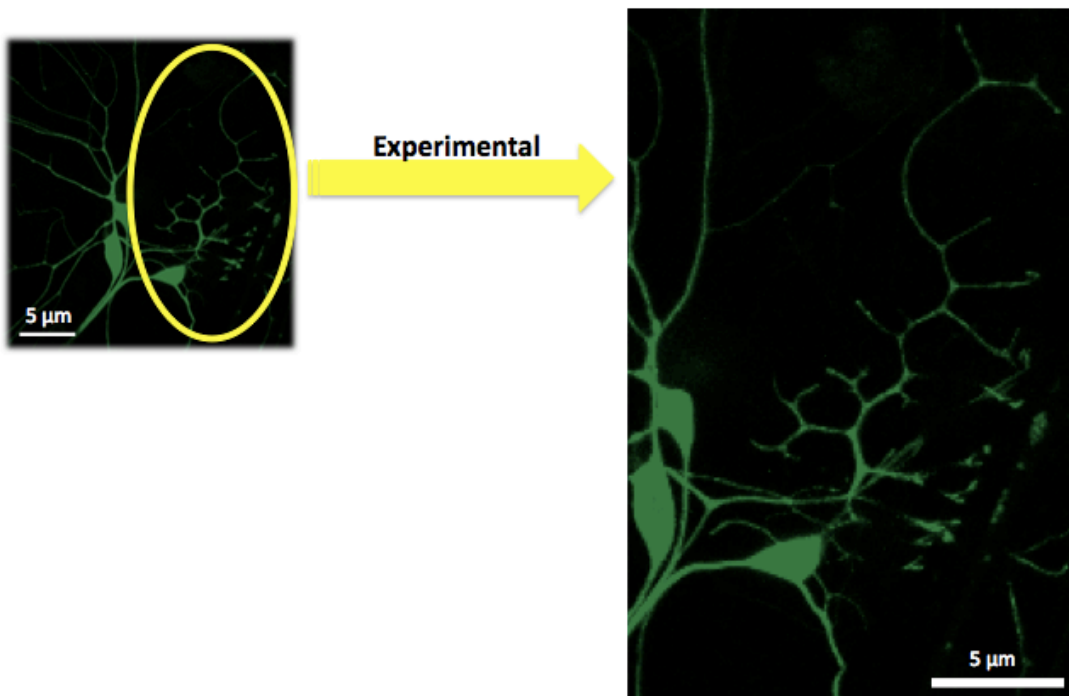


Figure 3: Dendrite Morphology in Experimental ddaE

This image is from live imaging with confocal microscopy. It represents the class I neuron's dendrites in a three-day old larvae from the experimental group. The expression of EB1-GFP is responsible for the green fluorescence. Like the control group, the ddaE depicted in this figure conserves the comb-like dendritic structure.

Moreover, an average number of 8.8 branch points was found in the experimental group and an average of 9.36 secondary branches for the control (figure 4), yielding a 5.98 percent difference. Based on the two-tailed t-test, this difference in the number of branch points was insignificant. The observed t-value of 0.838 was less than the critical t-value of 2.101 for an alpha level of 0.05 and 18 degrees of freedom.

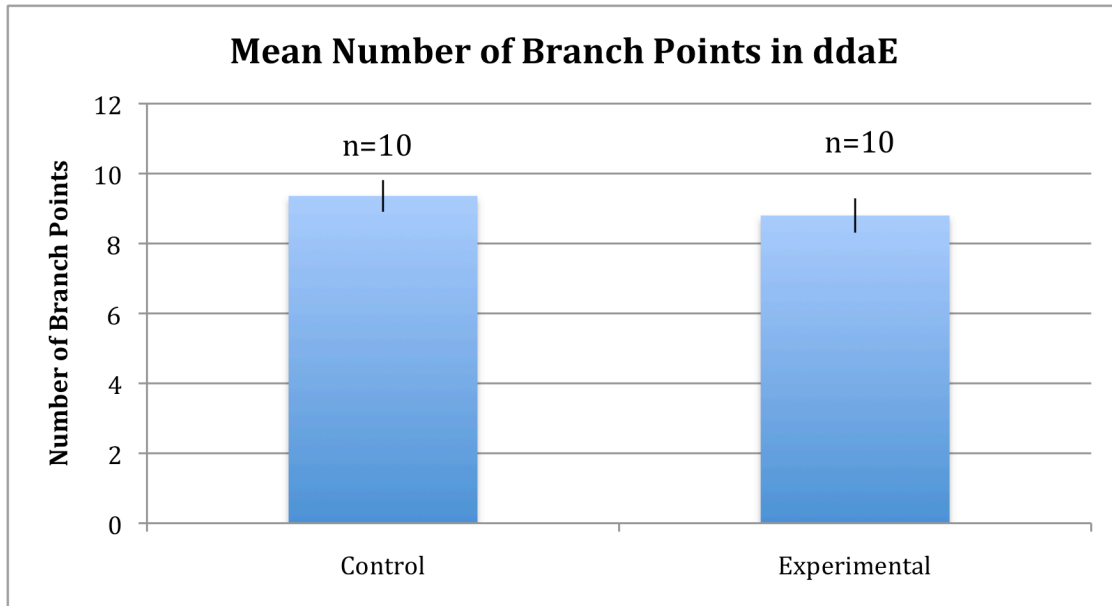


Figure 4: Branch Points in Class I Neuron

“n” is equal to the number of *Drosophila* larvae scored (one neuron per larvae). A sample size of 10 was used for the experimental group and the control group. Based on the experimental group’s results, the mean number of branch points was 8.8, and the variance was 2.4. The standard deviation was 1.549, and the standard error was 0.490. For the control group, the average number of branch points was 9.36, and the variance was 2.061. The standard deviation was 1.435, and the standard error was 0.454. The error bars in the graph refer to the standard error.

Since many of the images showed branches with curly tips, this observation was quantified. As figure 5 shows, an average of 0.2 curly tipped branches was found in the experimental group and an average of 0.18 in the control, yielding an 11.11% difference. According to the two-tailed t-test, this difference was insignificant. The observed t-value of 0.105 was less than the critical t-value of 2.101 for an alpha level of 0.05 and 18 degrees of freedom.

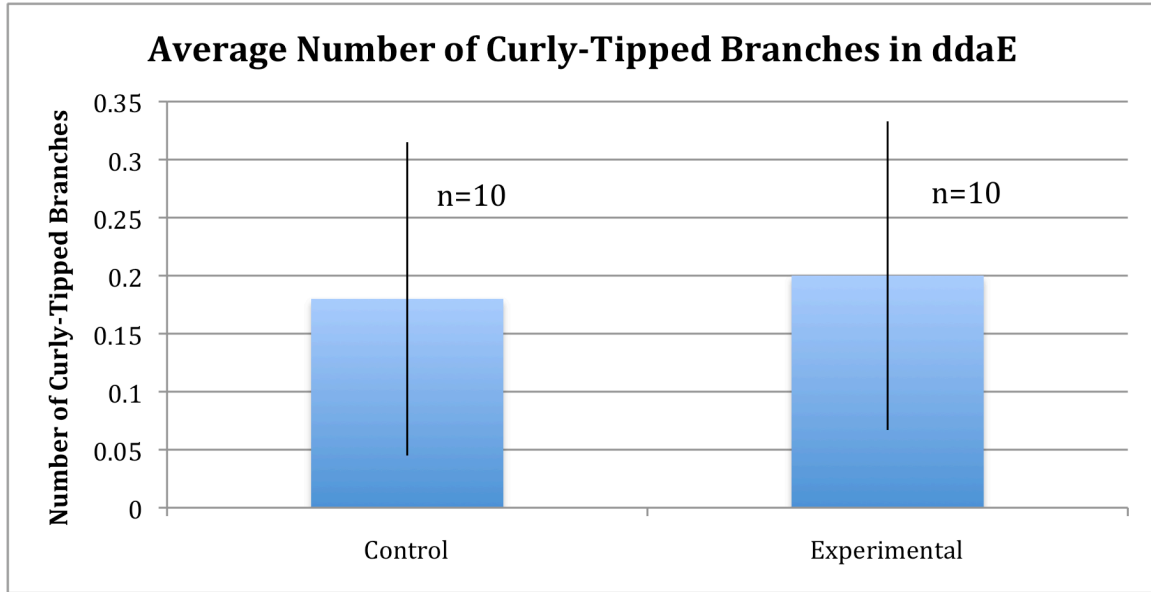


Figure 5: Prevalence of Curly-Tipped Branches

A sample size (n) of 10 was used for the experimental group and the control group. For the experimental group, the mean number of curly-tipped branches was 0.2, and the variance was 0.178. The standard deviation was 0.422, and the standard error was 0.133. For the control, the mean number of curly-tipped branches was 0.18, and the variance was 0.182. The standard deviation was 0.426, and the standard error was 0.135. The error bars refer to the standard error.

Moreover, dendrite reach was analyzed by measuring the linear distance from the junction between the cell body and the dendrite to the last branch point of the primary dendrite. An average dendritic reach of 28.78 μm was estimated for the experimental group and an average of 36.53 μm was found for the control (figure 6), giving a percent difference of 21.22%. The two-tailed t-test showed that this difference was insignificant. The observed t-value of 1.78 was less than the critical t-value of 2.101 for an alpha level of 0.05 and 18 degrees of freedom.

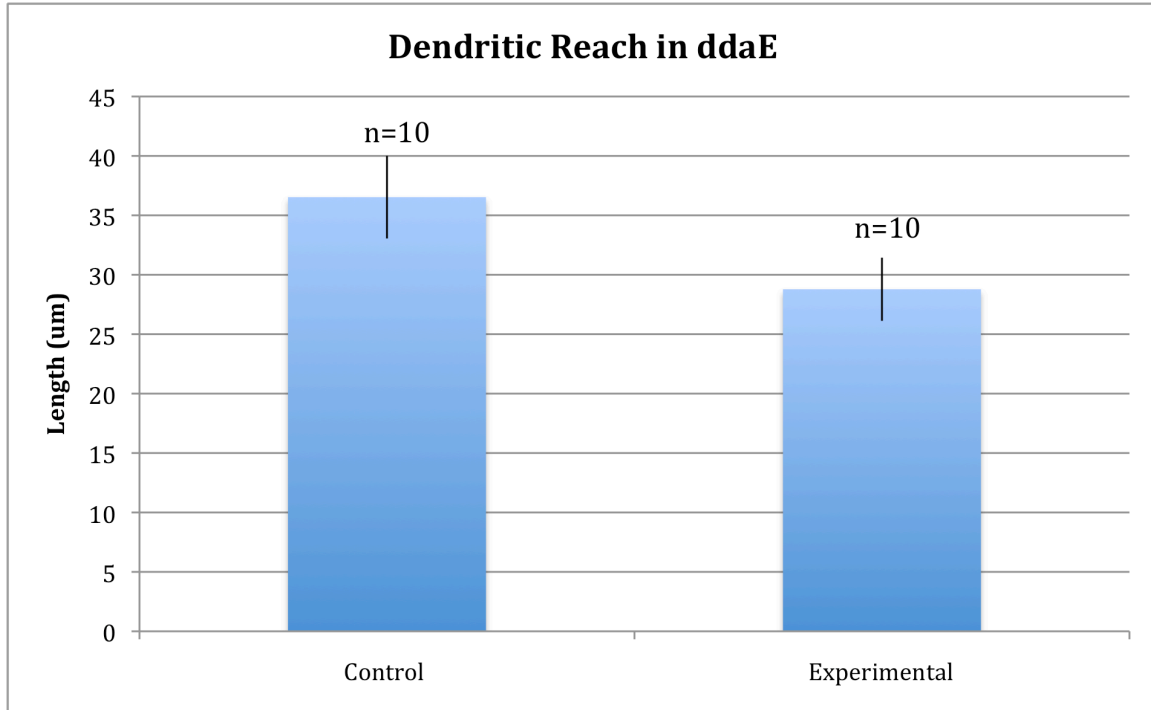


Figure 6: Dendritic Reach in Class I Neuron

"n" is equal to the number of *Drosophila* larvae scored (one neuron per larvae). A sample size of 10 was used for both the experimental group and the control group. For the experimental group, the average dendritic reach was 28.78, and the variance was 70.606. The standard deviation was 8.403, and the standard error was 2.657. For the control, the mean dendritic reach was 36.53, and the variance was 120.843. The standard deviation was 10.993, and the standard error was 3.476. The error bars indicate the standard error for each group.

Furthermore, an average length of 90.037 um was estimated for the primary dendrite in the control group and 76.866 um in the experimental group (figure 7), giving a percent difference of 14.628%. An outlier of 192.204 um was excluded in the calculation for the experimental group because the value was considerably different from the rest of the data set. When this value was included in the calculations, the standard deviation was 40 and the standard error was 12.646. However, excluding this single data point decreased the standard deviation and the standard error by a factor greater than 2, and consequently, this data point was defined as an outlier. According to the two-tailed t-test, this difference in the length of the primary dendrite of the ddaE was insignificant. The observed t-value of 1.332 was less than the critical t-value of 2.110 for an alpha level of 0.05 and 17 degrees of freedom.

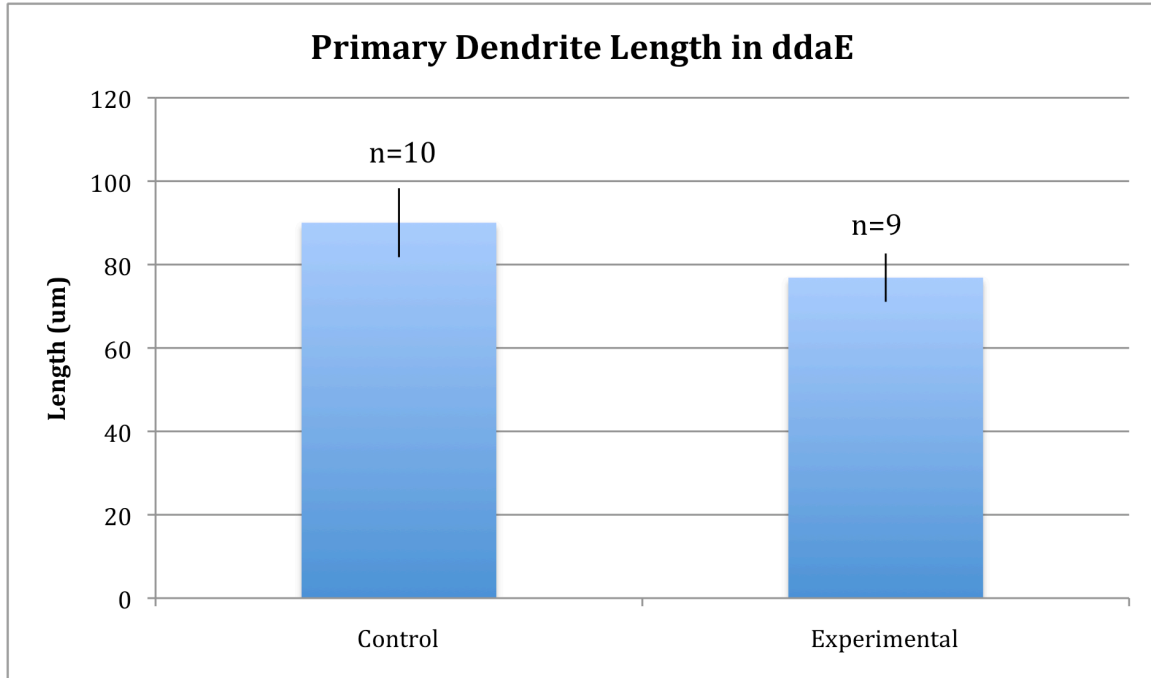


Figure 7: Primary Dendrite Length in the Class I Neuron

"n" is equal to the number of *Drosophila* larvae scored (one neuron per larvae). A sample size of 9 was used for the experimental group, and the sample size for the control group was 10. For the experimental group, the average dendrite length was 76.866, and the variance was 269.318. The standard deviation was 16.411, and the standard error was 5.802. For the control group, the mean dendritic length was 90.037 um, and the variance was 684.063. The standard deviation was 26.155, and the standard error was 8.271. The error bars indicate the standard error in each group.

Thus, dendrite morphology and growth pattern were not significantly altered in the class I neuron when the microtubule orientation is altered from minus-end-out to about evenly mixed. The mean length of the primary dendrite, dendritic reach, and the number of branch points and curly-tipped branches did not change considerably.

Microtubule polarity affects the abundance of mobile endosomes and the direction of the endosome trafficking

While dendrites and axons differ in their microtubule orientation, they are also unique with respect to the organelles they contain. Unlike axons, dendrites have organelles, such as the rough endoplasmic reticulum, polyribosomes, and Golgi outposts (Conde *et al.*, 2009), which collaborate to form an endomembrane system. Endosomes,

which are membrane-bound compartments, play an important in sorting and transport between these different organelles and the plasma membrane in this system (Campbell *et al.*, 2008). Moreover, endosomes control the membrane supply of dendrites. Thus, they are a distinguishing characteristic of dendrites. Additionally, endosomes bind to and travel along microtubules, and molecular motor proteins are responsible for mediating this movement (Murray *et al.*, 2003).

Therefore, the goal of this next experiment was to examine endosome trafficking in the main trunk of the class I neuron's dendrite when the orientation was changed from minus-end-out to evenly mixed. The hypothesis was that changing microtubule orientation would affect the direction of endosome movement in dendrites; although transport would still occur, the efficiency was expected to decrease. Since kinesin motor proteins walk towards the plus-end of a microtubule, it was hypothesized that the control group would have a majority of the endosomes in the dendrite moving towards the cell body. However, after knocking down the Kap3 levels with RNAi, the introduction of more plus-end-out microtubules in the dendrite was expected to cause more endosomes to be transported away from the cell body. Theoretically, with an evenly mixed microtubule orientation, the experimental group should have about an equal number of endosomes moving towards and away from the soma, whereas the control group should have cargo transport in their minus-end-out microtubules predominately directed towards the cell body.

The sample size was 29 for the control group (figure 8) and 30 fruit flies for the experimental group (figure 9). Each individual data point corresponds to a unique neuron from a distinct larva; no two neurons were imaged from the same larvae. Videos that

were not focused or unclear continuously were discarded, resulting in the uneven number of control and experimental samples. All the data was double-checked.

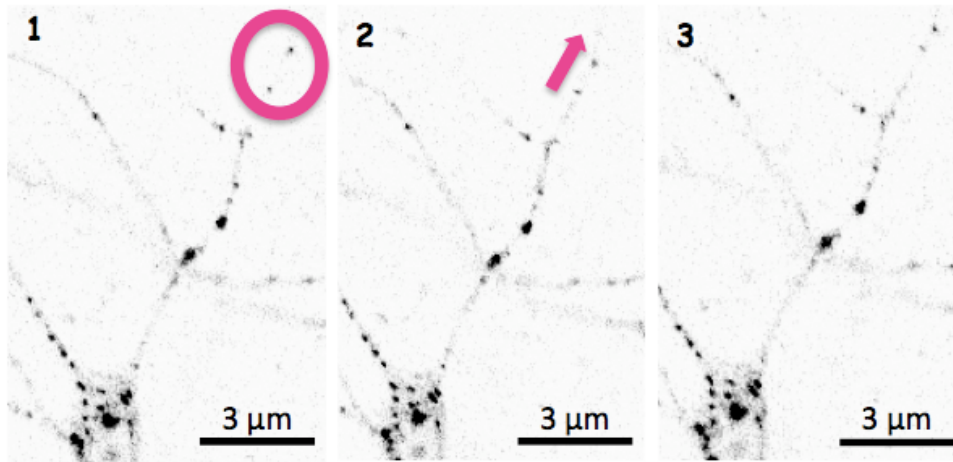


Figure 8: Endosome Trafficking in Control *ddaE*

The image of the class I neuron in a three-day old *Drosophila* larvae was taken during live imaging using a confocal microscope and modified to gray-scale settings in Image J. The cell body of the class I neuron is positioned at the bottom of the image, and the dendritic branches extend upward. The solid, black dots are endosomes in the dendrites. In the first image, the pink circle indicates the two endosomes in the comb dendrite that were tracked in this series of images. The pink arrow in the second image points in the direction that the lower comet in the pink circle had traveled. Finally, by the third image, the lower comet had moved close enough to the unmoving endosome (positioned further in the pink circle in image 1) to almost overlap it completely.

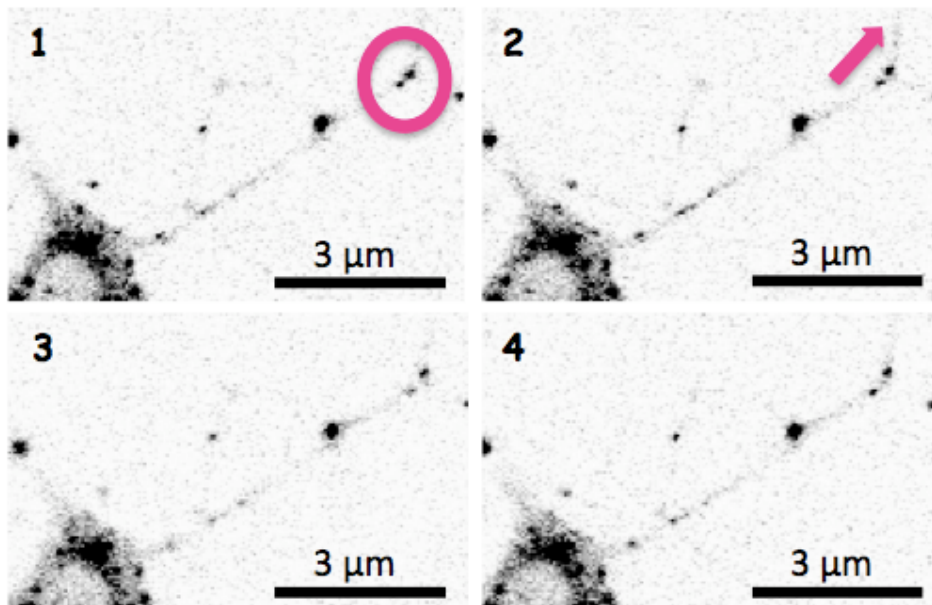


Figure 9: Endosome Trafficking in Experimental *ddaE*

The image of the class I neuron in a three-day old *Drosophila* larvae was taken during live imaging using a confocal microscope and modified to gray-scale settings in Image J. The cell body of the class I neuron is positioned at the bottom left side of each image, and the dendritic branches extend upward. The solid, black dots are endosomes in the dendrites. In the first image, the pink circle indicates

the two endosomes located in the comb dendrite that were tracked in the series of images. The pink arrow in the second image points in the direction that the comet further up in the pink circle had traveled relative to the unmoving endosome positioned below it. The third and fourth images show that the distance between these two endosomes increased as the top comet moved farther away.

However, the results did not support the hypothesis. Summing the endosomes moving towards the soma in all the 29 control units gave 133 endosomes in total, while a similar quantification for endosomes moving away from the soma gave 149 endosomes (figure 10). In other words, 47.16% of control endosomes moved towards the soma, while 52.84% moved away (figure 11), leading to a ratio of 0.893 endosomes towards versus away the soma (figure 12). Likewise, the total number of endosomes moving towards the soma in the 30 experimental units was 79 data points or 53.02%, compared to the 70 endosomes, or 46.98%, moving away from the soma. Therefore, the experimental group had a ratio of 1.13 endosomes towards versus away the soma.

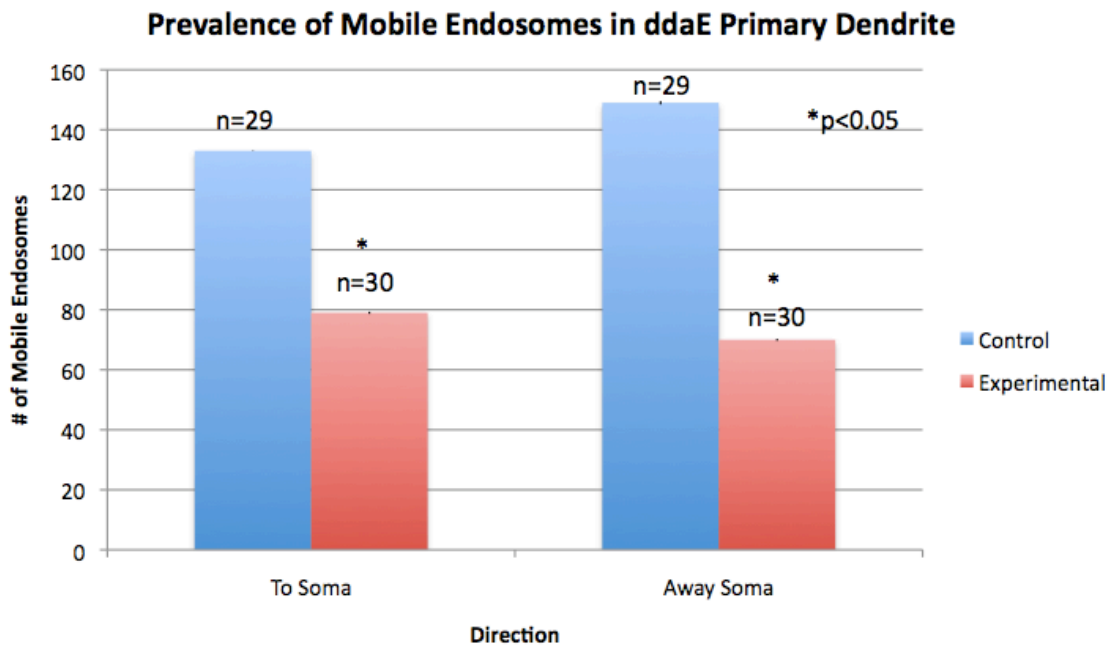


Figure 10: Number of Mobile Endosomes in the Primary Dendrite of the Class I Neuron

The graph is based on the data collected from live-imaging 29 control *Drosophila* larvae and 30 experimental larvae. “n” is equal to the number of *Drosophila* larvae scored (one neuron per larvae). The “To Soma” and “Away Soma” data was taken from the same neurons for each group. For the “To Soma” category of the control group, the mean number of mobile endosomes was 4.586, and the variance was 0.218. The standard deviation was 0.467, and the standard error as 0.0867. For the “Away Soma” of the

control group, the mean number of mobile endosomes was 5.138, and the variance was 9.123. The standard deviation was 3.020, and the standard error was 0.561. In the “To Soma” category of the experimental group, the average number of mobile endosomes was 2.633, and the variance was 3.620. The standard deviation was 1.903, and the standard error was 0.347. Lastly, for the “Away Soma” category of the experimental group, the average number of mobile endosomes was 2.333, and the variance was 3.471. The standard deviation was 1.863, and the standard error was 0.340. The error bars refer to the standard error, and the asterisk indicates a significant difference between the control and experimental groups.

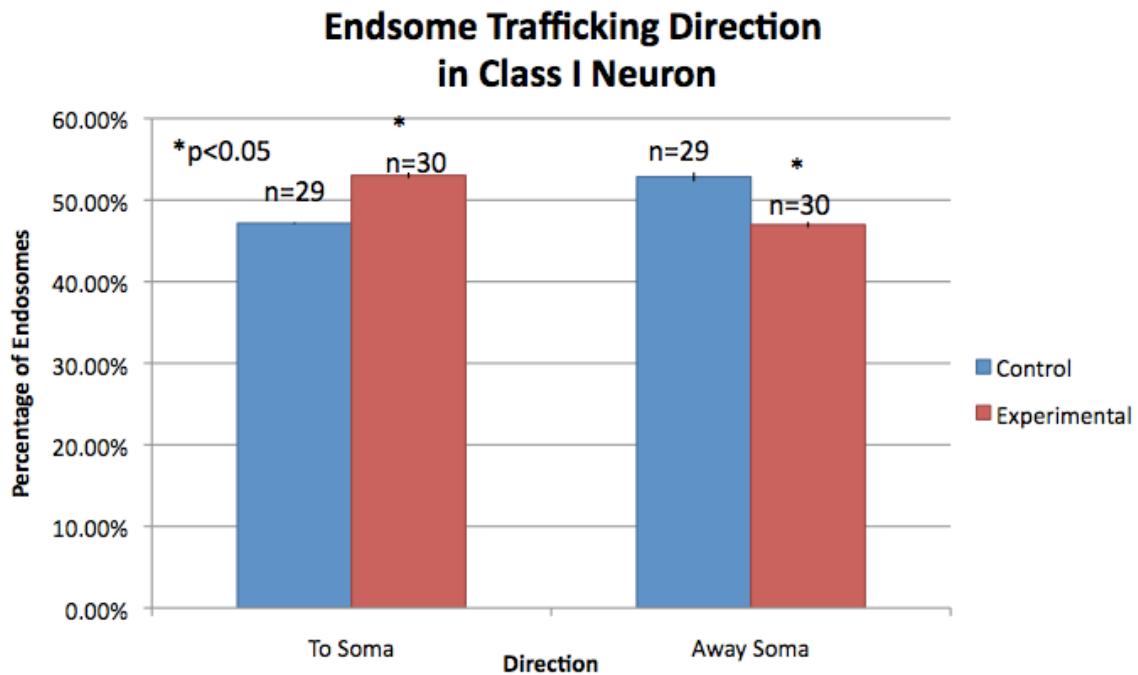


Figure 11: Percentage of Directional Trafficking by Endosomes

The graph is based on the total number of mobile endosomes presented in the figure 10. “n” is equal to the number of *Drosophila* larvae scored (one neuron per larvae). The “To Soma” and “Away Soma” data was taken from the same neurons for each group. The percentage of transport in each direction was calculated by dividing the number of endosomes traveling in that direction by the total number of endosomes present in either in the control group or the experimental group. This proportion was multiplied by 100 to yield the percentage. The graph shows that a greater proportion of mobile endosomes were traveling towards the soma in the experimental group, compared to the control group. As a result, a larger percentage of endosomes in the control group were found to be moving away from the soma. The error bars refer to the standard error, and the asterisk indicates a significant difference between the control and experimental groups.

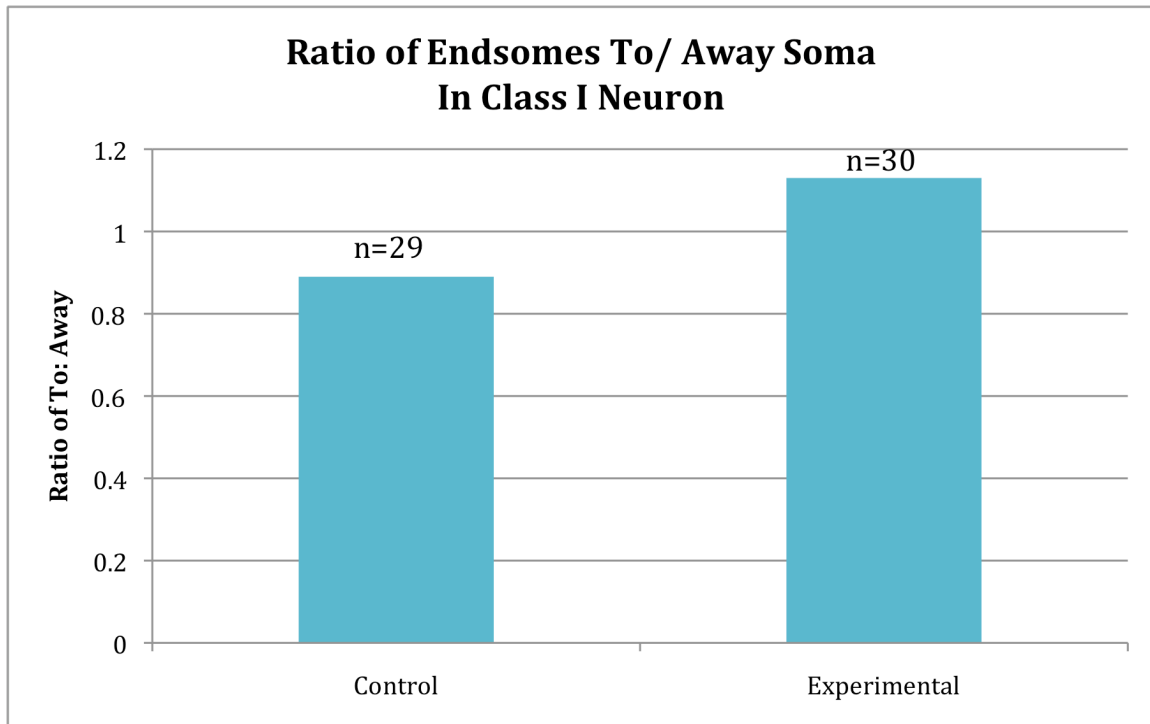


Figure 12: Ratio of Endosomes Traveling Towards and Away from the Soma

The graph is based on the total numbers of mobile endosomes traveling through the dendrites of a class I neurons, which was depicted in figure 10. “n” is equal to the number of *Drosophila* larvae scored (one neuron per larvae). For both the control and experimental groups, the total number of endosomes traveling towards the soma was divided by the total number moving away from the cell body to give the ratio of endosomes trafficked in either direction. Since this ratio for the control group was less than 1, a greater number of endosomes were traveling away from the soma in the control. The ratio for the experimental group was greater than 1, indicating that a larger number of mobile endosomes were heading towards to soma in the experimental group.

The ratios of the two groups differ by 27% difference. By comparing the control and experimental groups, it can be found that the ratio of endosomes to and away from the soma was 5.86% greater in the experimental group than the control; 5.86% more dots moved towards the soma than away in the experimental group compared to the control.

According to the two-tailed t-test, the difference in the prevalence of mobile endosomes traveling in either direction was significant. When the number of endosomes traveling towards the soma was compared between the control and experimental groups, the observed t-value was 5.372. At an alpha level of 0.05 and 57 degrees of freedom, the critical t-value was 2. Since the observed t-value was greater than the critical t-value, the null hypothesis was rejected, and a significant difference between the two groups was

concluded. Likewise, when the number of endosomes traveling away from the soma was compared between the control and experimental groups, the observed t-value was found to be 3.385. Since this is greater than the critical t-value of 2, the difference was determined to be significant.

A noteworthy difference is also evident in the magnitude of the total number endosomes found trafficking in the class I neuron. While a total number of 282 endosomes were counted in all the larvae of the control group, a sum of 149 endosomes was found in all the experimental larvae (figure 13). In other words, altering the microtubule orientation in the dendrites of the class I neuron from minus-end out to evenly mixed resulted in a down-regulation of endosome trafficking by a factor of 1.89. According to the two-tailed t-test, this difference was significant. The observed t-value of 2.825 was greater than the critical t-value of 2 for an alpha level of 0.05 and 57 degrees of freedom.

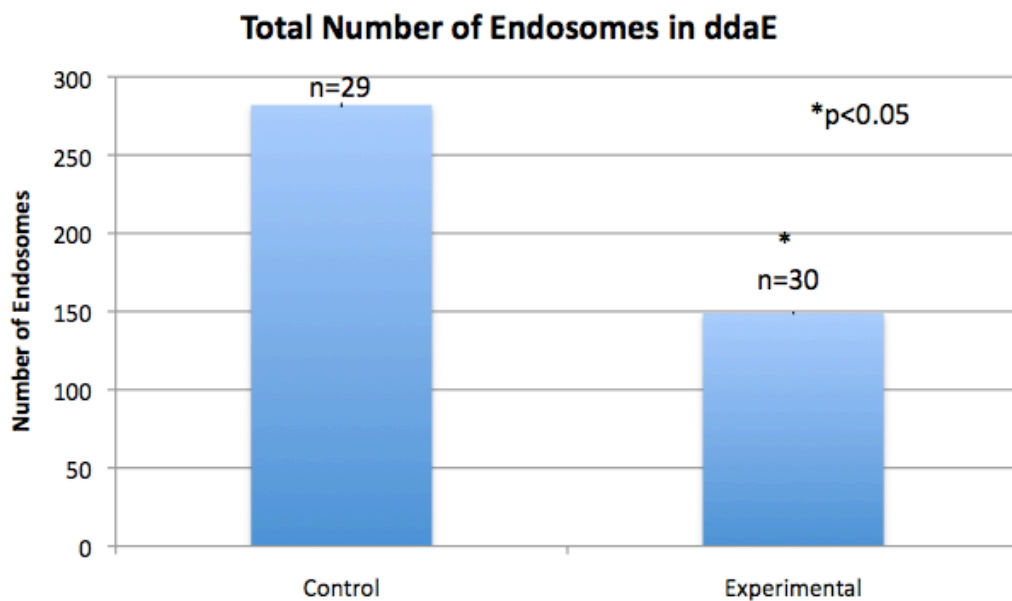


Figure 13: Total Quantity of Mobile Endosomes in the Class I Neurons

The graph represents the total number of mobile endosomes counted in 29 control larvae and 30 experimental larvae using the data collected from live imaging with confocal microscopy. "n" is equal to the number of *Drosophila* larvae scored (one neuron per larvae). Almost twice as many endosomes

are present in the control group, compared to the experimental group. For the control group, the mean number of endosomes was 9.724, and the variance was 64.569. The standard deviation was 8.035, and the standard error was 1.492. For the experimental group, the mean number of endosomes was 4.967, and the variance was 19.9. The standard deviation was 4.461, and the standard error was 0.814. The error bars refer to the standard error, and the asterisk indicates a significant difference between the control and experimental groups.

Thus, the hypothesis that the removal of Kap3 affects the direction of endosome transport of the class I neuron was correct. After the microtubule orientation was alerted from minus-end-out microtubules to about evenly mixed, the direction of endosome movement changed significantly. Moreover, disrupting the microtubule orientation caused a significant decrease in the total number of mobile endosomes throughout the primary dendrite of the ddaE. This unexpected difference was clearly evident from both qualitative assays of the time series videos from live imaging with confocal microscopy as well as subsequent quantitative analyses.

Microtubule polarity does not influence overall mitochondrial distribution, but affects branch point occupancy

Another organelle that is essential for neuronal differentiation and survival is the mitochondria. Oxidative phosphorylation of ATP by mitochondria is required to meet the high-energy demands of neurons. Inefficient mitochondrial transport can cause metabolic deficiencies, oxidative damage, excitotoxicity, and apoptosis that can result in muscular dystrophy, neuropathy, paraplegia, and neurodegeneration. This critical transport of mitochondria occurs along microtubule tracks and is mediated by molecular motors, such as kinesin and dynein proteins (Zinsmaier *et al.*, 2008).

Therefore, a third experiment was designed to examine the effects of disrupting minus-end-out microtubule orientation on the mitochondrial distribution in dendrites. It was hypothesized that the mixing the microtubule orientation would alter the distribution

of mitochondria in the class I neuron dendrites (figure 14). More specifically, introducing additional dendritic plus-end-out microtubules using Kap3RNAi would give kinesins more opportunities to transport mitochondria into the dendrites. Therefore, it was hypothesized that the experimental groups would have a greater number of mitochondria in its dendrites, compared to the control group.

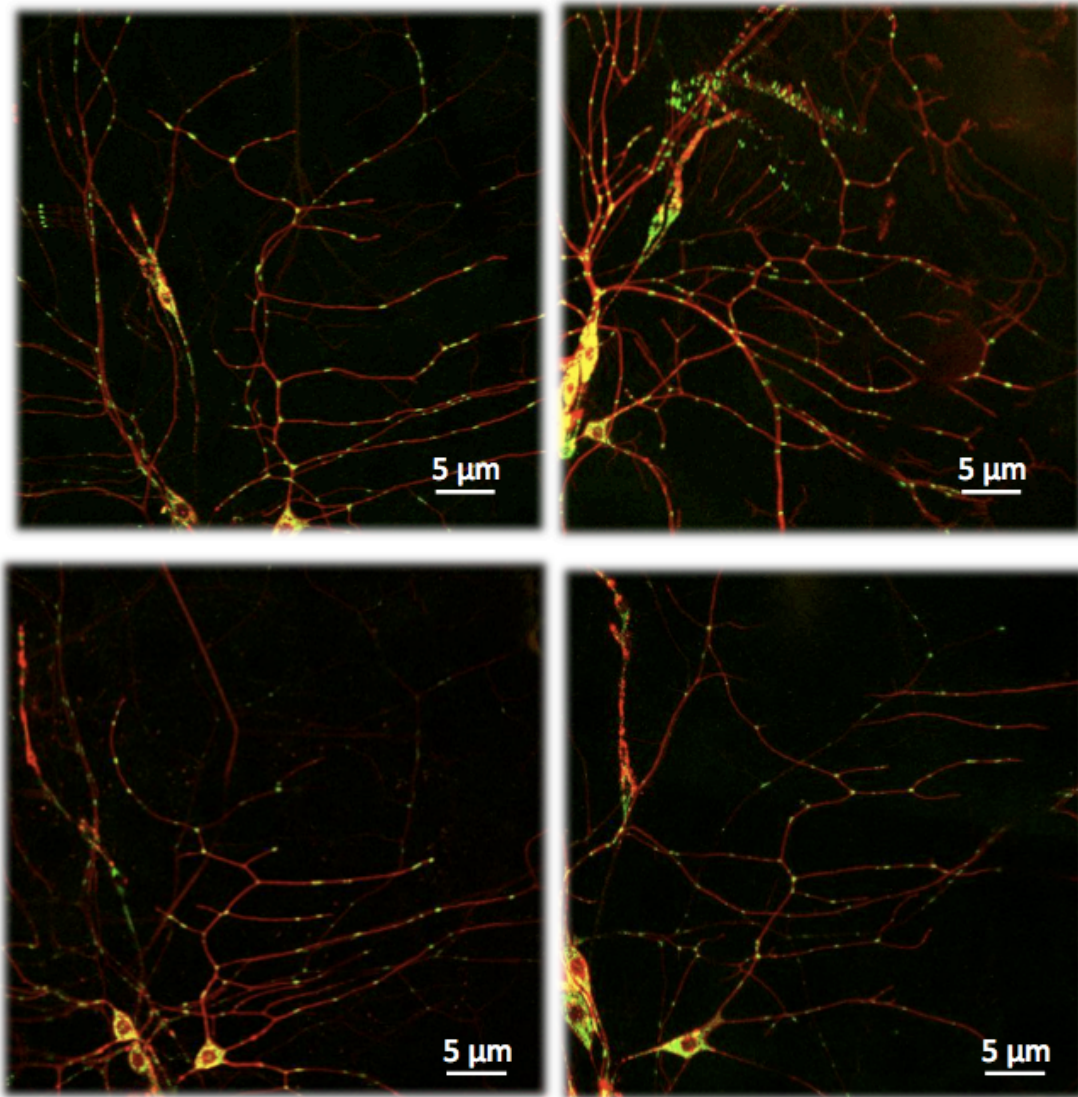


Figure 14: *ddaE* Mitochondrial Distribution in Control & Experimental Groups

These images of the class I neuron were obtained from live imaging 3-day old *Drosophila* larvae using confocal microscopy. The top two images are from the control group, and the lower two images are from the experimental group. The class I neuron is positioned on the right side of each image and can be easily distinguished by its comb dendrite. The mitochondria were labeled with mito-green fluorescent protein. mCD8-red fluorescent protein localizes on the plasma membrane and was used to outline the structure of the dendritic branches. Mitochondria in the primary dendrite and the secondary dendrites of the class I neuron were counted in this assay.

For the quantification of the mitochondria in the primary dendrite (figure 15), the sample size of 22 was used for the control group and 21 for the experimental group. A maximum of 12 branch points and a minimum of 4 branch points were found in all the data. The average number of mitochondria throughout the primary dendrite was found to be 16.57 for the control and 14.52 for the experimental group, yielding a 12.7% difference in the average number of mitochondria in the main branch. According to the two-tailed t-test, this difference was significant. The observed t-value of 2.188 was greater than the critical t-value of 2.020 at an alpha level of 0.05 and 41 degrees of freedom.

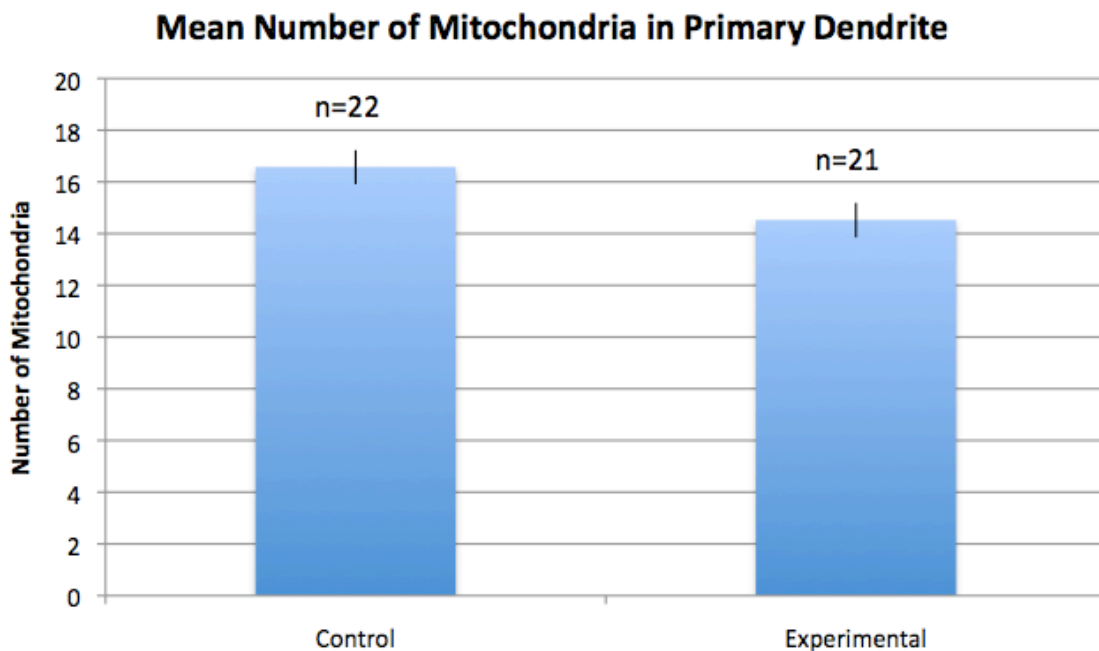


Figure 15: Mean Number of Mitochondria in Primary Dendrite of *ddaE*

The results in this graph are based on data collected from live imaging 3-day old *Drosophila* larvae. "n" is equal to the number of *Drosophila* larvae scored (one neuron per larvae). The graph depicts the average number of mitochondria in the primary dendrite of the class I neuron for the control and experimental groups. The sample size for the control group was 22, and the sample size for the experimental group was 21. The average number of mitochondria for the control group was 16.57, and the variance was 9.5. The standard deviation was 3.082, and the standard error was 0.657. For the experimental group, the mean number of mitochondria in the primary dendrite was 14.52, and the variance was 9.362. The standard deviation was 3.06, and the standard error was 0.668. The error bars indicate the standard error.

When calculating the average number of mitochondria per unit length (figure 16), a sample size of 16 was used for both groups. The sum of the numbers of mitochondria in the primary dendrite and the secondary dendritic branches was divided by the total length of the primary and secondary dendrites. An average of 0.0557 mitochondria per μm was estimated for the experimental group, and an average of 0.0540 mitochondria per μm was found for the control group, yielding a 3.25% difference. In the two-tailed t-test, the observed t-value of 0.360 was not greater than the critical t-value of 2.042 at an alpha level of 0.05 and 30 degrees of freedom. Therefore, the number of mitochondria per unit length throughout the dendrite does not change significantly upon altering microtubule orientation.

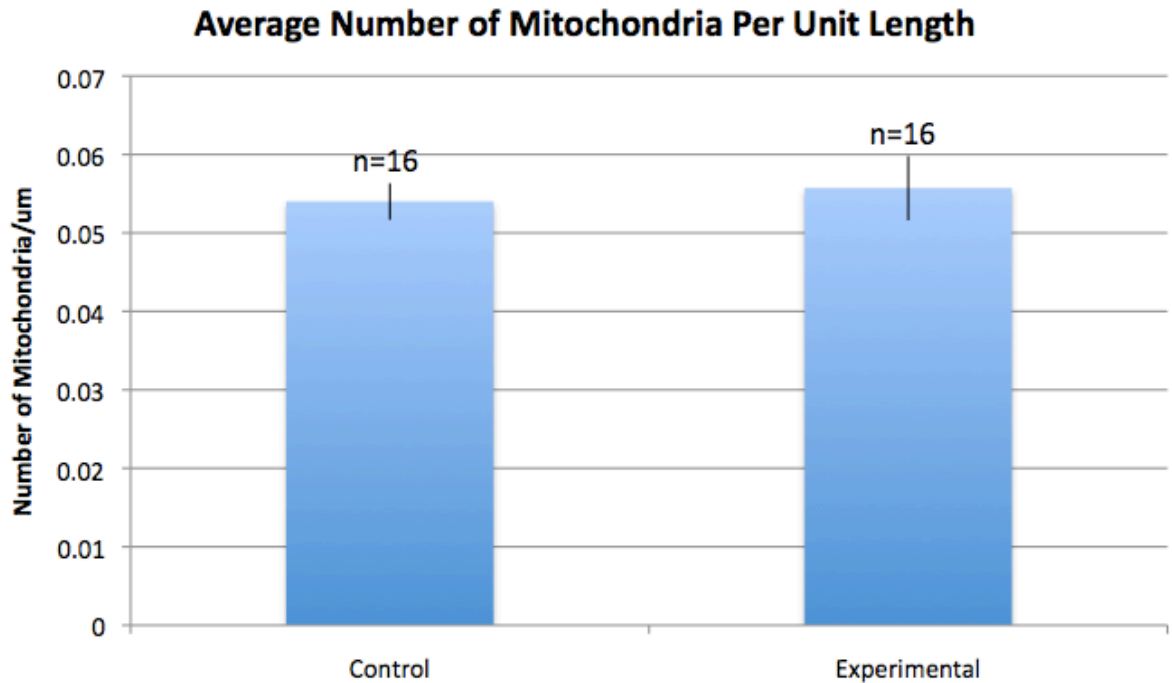


Figure 16: Mean Number of Mitochondria Per Unit Length

The results presented in this graph are based on data collected from live imaging 3-day old *Drosophila* larvae. The graph depicts the average number of mitochondria counted throughout the entire Class I neuron divided by the total length of the ddaE. The sample size (n) for the control and the experimental groups was 16. The average number of mitochondria per unit length for the control group was 0.0540 mitochondria per micrometer, and the variance was 0.0000872. The standard deviation was 0.00934, and standard error 0.00233. For the experimental group, the mean number of mitochondria per micrometer was 0.0557, and the variance was 0.000269. The standard deviation was 0.0164, and the standard error was 0.0041. The error bars indicate the standard error.

Furthermore, an average of 1.17 mitochondria were found per branch point in the primary dendrite of the class I neuron of the control group and 0.97 mitochondria per branch point in the experimental group (figure 17). The sample size was 22 larvae for the control group and 21 larvae for the experimental group. A 47% difference in the average number localized at the branch points was found. There were about twice as many mitochondria at the branch points in my control group compared to my experimental. However, the reliability of these results is questionable because manually tallying the endosomes at each branch point may have been subjective. If several mitochondria were overlapping each other at a single branch point, fewer mitochondria would have been tallied than the true value, and the results would then be an underestimate. Furthermore, according to the two-tailed t-test, the difference in the number of mitochondria localized to branch points was insignificant. The observed t-value of 1.219 was less than the critical t-value of 2.020 at an alpha level of 0.05 and 41 degrees of freedom.

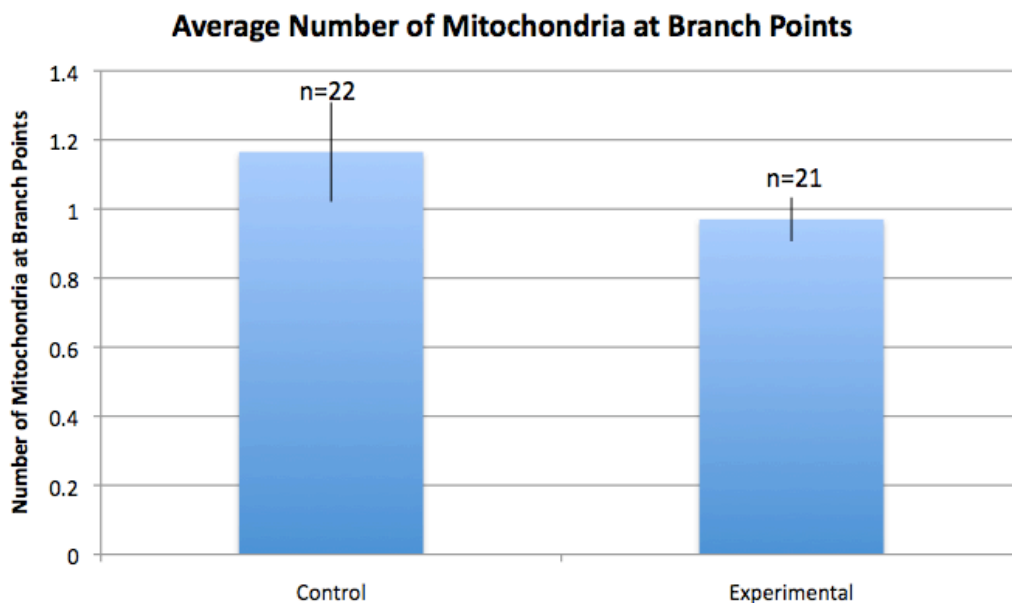


Figure 17: Mean Number of Mitochondria at Branch Points

The results in this graph are based on data collected from live imaging 3-day old *Drosophila* larvae. The graph depicts the average number of mitochondria per branch point in the primary dendrite

of the Class I neuron. “n” is equal to the number of *Drosophila* larvae scored (one neuron per larvae). The sample size was 22 larvae for the control group and 21 larvae for the experimental group. For the control group, the average number of mitochondria at branch points was 1.165, and the variance was 0.457. The standard deviation was 0.676, and the standard error was 0.144. For the experimental group, the average number of mitochondria per branch point was 0.97, and the variance was 0.844. The standard deviation was 0.290, and the standard error was 0.0634. The error bars show the standard error for each group.

Moreover, the average number of branch points occupied with at least one mitochondrion was found to be 0.91 for the control and 0.82 for the experimental group (figure 18). The sample size was 22 larvae for the control group and 21 larvae for the experimental group. As the two-tailed t-test showed, the 9.89 percent difference between the control group and the experimental group was significant. The observed t-value of 2.118 was greater than the critical t-value of 2.020 at an alpha level of 0.05 and 41 degrees of freedom. Therefore, the null hypothesis was rejected, and it was concluded that changing the microtubule orientation of dendrites from minus-end-out to about evenly mixed significantly decreases the branch point occupancy in the primary dendrite of the class I neurons of *Drosophila*.

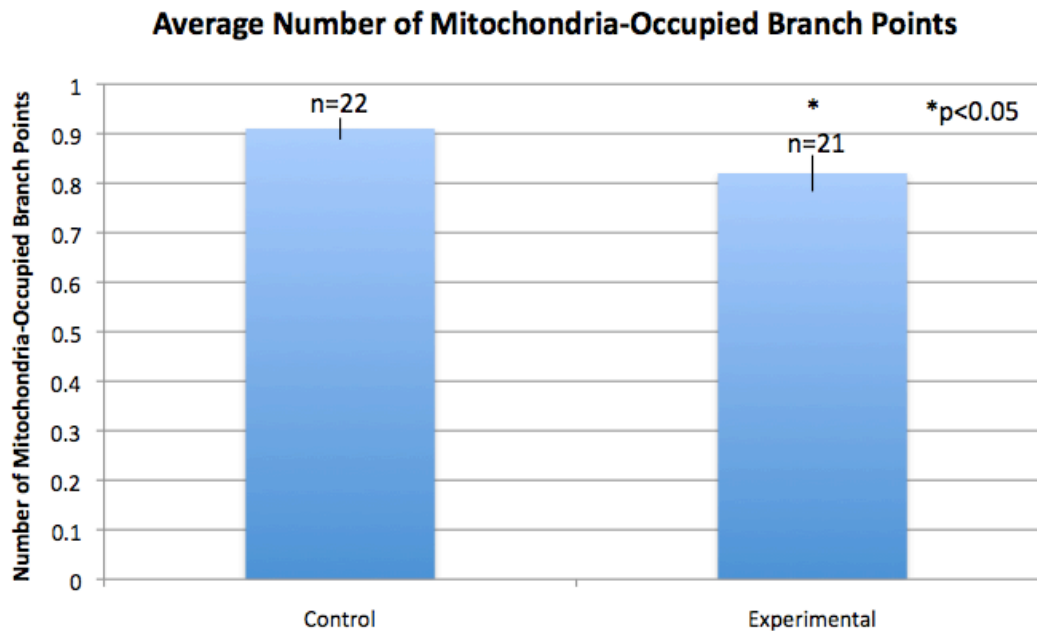


Figure 18: Mean Number of Branch Points Occupied with Mitochondria

The results in this graph are based on data collected from live imaging 3-day old *Drosophila* larvae. The graph depicts the average number of branch points in the primary dendrite of the Class I

neuron that were occupied with mitochondria. The sample size for the control group was 22, and the sample size for the experimental group was 21. For the control, the mean number of mitochondria-occupied branch points was 0.91, and the variance was 0.012. The standard deviation was 0.103, and the standard error was 0.022. For the experimental group, average number of mitochondria-occupied branch points was 0.82, and the variance was 0.0284. The standard deviation was 0.169, and the standard error was 0.0368. The error bars depict the standard error, and the asterisk indicates that a significant difference exists between the control and experimental groups.

Discussion

The purpose of this research was to learn about how microtubule polarity contributes to polarized trafficking of proteins and organelles in dendrites and, thus, their specialization in structure and function. Fluorescently tagged protein markers, RNAi, and confocal microscopy were used to examine how distinguishing characteristics of the class I neuron in *Drosophila melanogaster* dendrites was affected when microtubule orientation was changed from minus-end-out to about evenly mixed. Since previous research studies support the minus-end-out microtubule signature in *Drosophila* dendrites (Rolls *et al.*, 2007), it was hypothesized that altering the microtubule orientation would cause the ddaE dendrites to lose their typical shape and organelle distribution.

The first step was to examine the overall morphology of the class I neuron. Did the dendrite structure or growth pattern change in neurons with the introduction of more plus-end-out microtubules? According to the two-tailed t-tests, no significant phenotype was found. The comb-like shape of the neuron was conserved, and the number of branch points along the primary dendrite, length of the primary dendrite, dendritic reach, and prevalence of curly-tipped secondary branches were not considerably different between the control and experimental groups. Thus, altering microtubule polarity did not significantly affect dendrite morphology.

Since dendrites have specific proteins and organelles that are relatively scarce in axons (Craig *et al.*, 1994), the effect of microtubule polarity on this organelle trafficking and distribution within the dendrite was examined. Endosome movements were tracked throughout the primary dendrite of the class I neuron and quantified. Contrary to the hypothesis, 5.86% more endosomes moved towards the soma than away in the

experimental group compared to the control. According to the two-tailed t-test, this result was significant; the introduction of more plus-end-out microtubules in dendrites caused a statistically noteworthy increase in cargo transport towards the cell body. However, since this difference is small, further data collection and analysis may be necessary to increase the sample size and strengthen this conclusion.

Another unexpected phenotype observed significantly in the dendrites upon microtubule orientation mixing was the decrease in the total number of endosomes in the primary dendrite of the class I neuron by a factor of 1.89. Almost half as many endosomes were present in the dendrite after microtubule orientation was changed to evenly mixed. Several possibilities may explain this reduction in the abundance of mobile endosomes in the primary branch of the comb dendrite. For example, a change in microtubule polarity may have hindered endosomes from entering at branch points, but further live imaging and quantification to compare the prevalence of mobile endosomes in the secondary branches and their localization frequency at the branch points may aid in testing this hypothesis. Also, the altered microtubule orientation might have compromised the mobility of the endosomes already present in the primary dendrite. To evaluate this possible mechanism behind the down-regulation phenotype, quantification of the total number of mobile and immobile endosomes throughout the primary dendrite of the class I neuron may be useful.

Interestingly, according to previous research, disrupting endosomal function changes dendrite morphogenesis, including branch formation (Sweeney *et al.*, 2006). However, the results from this project showed that altering the minus-end-out microtubule signature of *Drosophila* dendrites changed the pattern of endosome transport

and distribution in the dendrite significantly, but not dendritic morphology. Since three-day old larvae were assayed in this project, one possible explanation for this difference in observations may be that any possible changes in dendrite morphogenesis might occur early on in the life cycle of the larvae and, by the third day of aging, the morphology may be modified to the normal phenotype of the comb dendrite that was seen in the control larvae in this project. Future experiments could track the changes in the morphology of dendrites during the first three days of aging to evaluate the plausibility of this explanation.

Additionally, the results from live imaging in this project showed that some endosomes raced towards and away from the cell body, while other moved at a much slower pace. If time permitted, further interesting questions could have also been pursued. For example, is the speed of the endosomes affected? Does the distance traveled by the endosomes change?

Mitochondria are also essential organelles for dendritic differentiation and survival, and they are transported with the aid of motor proteins (Zinsmaier *et al.*, 2008). Consequently, their distribution in the dendrite was investigated when microtubule orientation was mixed. Compared to the previous assay, the live imaging resolution for this experiment was much higher, and a large sample size was easily attained. According to the two-tailed t-test, the mean number mitochondria in the primary dendrite of the ddaE, the number of mitochondria per micrometer, and the number of mitochondria localized at the branch points were not significantly different between the control and experimental groups. Moreover, the quantification of the number of mitochondria concentrated at branch points may not be highly reliable because the Golgi clustered at

each branch point are difficult to distinguish apart; many could possibly be overlapping, which would explain the different sizes of the GFP-labeled Golgi beads that were observed at these branch points. Consequently, the data analysis design for this particular series of data was too weak to make a confident conclusion. More explicate labeling or tracking methods may be required to make a conclusion about the Golgi prevalence at branch points.

Interestingly, although the number of mitochondria per unit length in the class I neuron did not change significantly, the quantity of branch points occupied with mitochondria was significantly greater for the control compared to the experimental group. However, the 9.89 percent difference between the control group and the experimental group appears small, and more data may need to be collected to increase the sample size and strengthen this conclusion. As for endosome trafficking, the altered microtubule polarity may have compromised the transport of mitochondria in the comb dendrite. The cell body is responsible for synthesizing many proteins and organelles, including the mitochondria, and kinesin and dynein motors mediate the mitochondrial transport in neurons (Zinsmaier *et al.*, 2008). The addition of plus-end-out microtubules in the dendrite may have provided kinesin motors more opportunities to transport mitochondria a greater distance away from the cell body and towards the periphery of the neuron. As a result, the transport of fewer mitochondria may have terminated at the dendritic branch points, and instead, more mitochondria might have spread throughout the class I neuron. To further evaluate the potential contribution by kinesin motors to the phenotype in mitochondrial distribution, future research studies could test whether the number of mitochondria increases with distance from the cell body when the minus-end-

out microtubule orientation is changed to evenly mixed. Moreover, the change in microtubule orientation may have caused more mitochondria to localize between branch points, but further data quantification is needed to test this hypothesis.

Furthermore, a change in microtubule polarity could have hindered mitochondria from entering at branch points and resulted in the decreased localization of mitochondria at these branch points. If this were indeed the case, a greater number of mitochondria would have been restricted to the primary dendrite. However, according to the two-tailed t-test, the number of mitochondria in the primary dendrite did not change significantly after the microtubule orientation was altered. Therefore, this explanation may not be plausible.

Therefore, the experiments in this project have shed light on the role of microtubule polarity in polarized trafficking in dendrites. Altering microtubule orientation did not significantly affect dendritic morphology or growth pattern. However, the increase in endosome transport towards the soma and the down-regulation in the total quantity of endosomes in the class I neuron were statistically significant. Furthermore, the mean number of mitochondria in the primary dendrite, the number of mitochondria per unit length, and the number of mitochondria localized at branch points did not change considerably, but the prevalence of branch points occupied with at least one mitochondrion decreased significantly after microtubule orientation became evenly mixed. These results suggest that organelle transport to dendrites may not be hindered with a change in microtubule orientation; dendritic trafficking may not differ regardless whether the microtubule polarity is minus-end-out or evenly mixed. However, the results from the endosome trafficking assay seem to contradict this conclusion, and

consequently, more data needs to be collected from this experiment to increase the sample size and test this hypothesis more rigorously.

Further research is necessary to identify the mechanisms that contributed to the significant phenotypes in endosome trafficking and mitochondrial distribution. Experiments investigating the effect of disrupting the minus-end out microtubule orientation on Golgi localization, Rab-3 localization and neurotransmitter release, and atrial natriuretic factor distribution in the ddaE dendrites can also provide further insight into the role of microtubules polarity in directional transport in *Drosophila melanogaster* by testing whether axonal components are introduced into dendrites when plus-end-out microtubules are present in the dendrites. A deeper understanding of the contribution of microtubule polarity to polarized trafficking of organelles in the dendrites may aid in advancing research about the structural and functional specialization of dendrites as well as medical therapies for neurodegenerative diseases.

References

1. Anderson, R., Li, Y., Resseguie, M., and Brenman, J.E. (2005). Calcium/Calmodulin-Dependent Protein Kinase II Alters Structural Plasticity and Cytoskeletal Dynamics in *Drosophila*. *Journal of Neuroscience*. *25*, 8878-8888.
2. Baas, P.W., and Lin, S. (2010). Hooks and comets: The story of microtubule polarity orientation in the neuron. *Developmental Neurobiology*. *71*, 403-418.
3. Bartolini, F., and Gundersen, G.G., (2006). Generation of noncentrosomal microtubule arrays. *Journal of Cell Science*. *119*, 4155-4163.
4. Black, M.M., and Baas, P.W. (1989). The basis of polarity in neurons. *Trends in Neurosciences*. *12*, 211-214.
5. Burton, P.R. (1988). Dendrites of mitral cell neurons contain microtubules of opposite polarity. *Brain Research*. *473*, 107-115.
6. Conde, C., and Cáceres A. (2009). Microtubule assembly, organization and dynamics in axons and dendrites. *Nature Reviews Neuroscience*. *10*, 319-332.
7. Craig, A.M., and Banker, G. (1994). Neuronal Polarity. *Annual Review of Neuroscience*. *17*, 267-310.
8. Dietzl, G., Chen, D., Schnorrer, F., Su, K.C., et al. (2007). A genome-wide transgenic RNAi library for conditional gene inactivation in *Drosophila*. *Nature*. *448*, 151-156.
9. Grueber, B., Jan, L.Y., and Jan, Y.N. (2002). Tiling of the *Drosophila* epidermis by multidendritic sensory neurons. *Development*. *129*, 2867-2878.
10. Jimbo, T., Kawasaki, Y., Koyoma, R., Sato, R., Takada, R., Haraguchi, K., and Akiyama, T. (2002). Identification of a link between the tumour suppressor APC and the kinesin superfamily. *Nature Cell Biology*. *4*, 323-327.
11. Kuo, John. (2007). *Electron Microscopy: Methods and Protocols*, ed 2. Totowa: Humana Press. 2, 208.
12. Lansbergen, G., and Akhmanova. (2006). Microtubule plus end: a hub of cellular activities. *Traffic*. *7*, 499-507.
13. Lodish H., Berk, A., Zipursky S.L., et al. (2000). Kinesin, Dynein, and Intracellular Transport. In: *Molecular Cell Biology*, ed 4. New York: W.H. Freeman, 19.3.

14. Mattie, F. J., Rolls, M.M., and Stone, M.C. (2010). Directed Microtubule Growth, +TIPs, and Kinesin-2 Are Required for Uniform Microtubule Polarity in Dendrites." *Current Biology*. 20, 1-9.
15. Murray, J. W., Bananis, E., and Wolkoff, A.W. (2000). Reconstitution of ATP-dependent Movement of Endocytic Vesicles Along Microtubules In Vitro: An Oscillatory Bidirectional Process. *Molecular Biology of the Cell*. 11, 419-433.
16. Murray, J W., and Wolkoff, A.W. (2003). "Roles of cytoskeleton and motor proteins in endocytic sorting." *Adv Drug Deliv Rev*. 55, 1385-1403.
17. Oertle, T., Klinfer, M., Stuermer, C.A.O., and Martin, S. (2003). A reticular rhapsody: phylogenic evolution and nomenclature of the RTN/Nogo gene family. *The Journal of the Federation of American Societies for Experimental Biology*. 17, 1238-1247.
18. Perrone-Capano, C., and Umberto, D.P. (2000) Genetic and epigenetic control of midbrain dopaminergic neuron development. *International Journal of Developmental Biology*. 44, 679-687.
19. Rogers, S.L., Rogers, G.C., Sharp, D.L., and Vale, R.D., (2002). Drosophila EB1 is important for proper assembly, dynamics, and positioning of mitotic spindle. *Journal of General Physiology*. 158, 873-884.
20. Rolls, M. M., Satoh, D., and Clyne, P.J. (2007). Polarity and intracellular compartmentalization of Drosophila neurons. *Neural Development*. 2, 1-14.
21. Rolls, M. M. (2010). Neuronal polarity in Drosophila: sorting out axons and dendrites. *Developmental Neurobiology*.
22. Stepanova, T., Slemmer, J., Hoogenraad, C. C., Lansbergen G., Dortland B., De Zeeuw, C. I., Grosveld, F., van Cappellen, G., Akhmanova A., and Galjart, N. (2003). Visualization of microtubule growth in cultured neurons via the use of EB3-GFP (end-binding protein 3-green fluorescent protein). *Journal of Neuroscience*. 23, 2655-2664.
23. Stone, M. C., Melissa M. M., and Roegiers, F. (2008). Microtubules Have Opposite Orientation in Axons and Dendrites of Drosophila Neurons. *Molecular Biology of the Cell*. 19, 4122-4129.
24. Sweeney, N.T., Brenman, J.E., Jan Y.N., and Gao, F.B. (2006). The coiled-coil protein shrub controls neuronal morphogenesis in Drosophila. *Current Biology*. 16, 1006-1011.

25. Zinsmaier, K. E., Babic, M., and Russo, G.J. (2008). Mitochondrial Transport Dynamics in Axons and Dendrites. *Results and Problems in Cell Differentiation*. 48, 361-362.

Vita

Manpreet Parmar



Penn State University
University Park, PA, 16802
mqp5088@psu.edu

113 Alma Mater Drive
State College, PA, 16803
(732)-832-9208

Personal Information

DOB: 05/19/1990

Place of Citizenship: United States of America

Education

Bachelors of Science in Biology (Vertebrate Physiology Option)
Pennsylvania State University, Spring 2012

Honors in Biology

Thesis Title: The Function of Microtubule Polarity in *Drosophila* Dendrites

Thesis Supervisor: Melissa Rolls

Honors and Awards

- Schreyer Ambassador Travel Grant for London Study Tour (Theatre 497H)
- Penn State Phi Eta Sigma Honors Society
- Alpha Epsilon Delta National Health Professions Honor Society
- Dean's List for all semesters at Penn State University Park
- Elizabeth S. and William Henry Gaeckle Alumni Memorial Scholarship (August 2008-May 2012)
- Bank of America Joe Martin Scholarship for all semesters (August 2008-May 2012)
- Schreyer Honor College Grant for Homes of the Indian Nation Service-Learning Program (July-August 2009)

- Penn State Schreyer Honors College Summer Research Grant (May-July 2009)
- Pennsylvania Space Grant by Women in Science and Engineering Research Program (August 2008 – August 2009)

Association Memberships

- Volunteered at the Homes of the Indian Nations (HOINA) in Vishakhapatnam, Andhra Pradesh, South India (July 2009 – August 2009)
- Prepared for and participated in 5K races to raise funds for Thon and advocate for the fight against racism (2008-2012)
- March of Dimes Fundraiser & Walk-a-thon (April 2004- April 2012)
- Leukemia & Lymphoma Fundraiser & Light the Night Walk-a-thon (October 2004-October 2011)
- Schreyer Honors College Student Council: Academic Committee (September 2008-May 2012)
- Badminton Club (September 2008-Present)
- South Asian Student Association (September 2008 – Present)
- Springfield Thon (September 2008-December 2009)
- Volunteer in the Emergency Department at Mount Nittany Medical Center: 54.7 hours earned (December 2008 – Present)
- Volunteered on the geriatric floor of the Raritan Bay Medical Center in Old Bridge, New Jersey: 450 hours earned (September 2004 – February 2008)

Research Experience

In January 2009, I joined Dr. Roll's molecular biology lab, which focuses on the study of microtubule orientation, polarized trafficking, and injury in neurons of *Drosophila melanogaster*. As an undergraduate researcher, I have become skilled in raising fruit flies and analyzing their nervous system development using confocal microscopy. I have also learned about safety techniques, lab etiquette, and waste disposal. I have assayed the class I neuron when microtubule orientation is changed from minus-end-out microtubules to evenly mixed. I am particularly curious about how proteins and organelles are moved along the primary and secondary branches of the ddaE dendrite.

Teaching Experience

- Tutoring in math, science, and English for high school students
- Private Instructor for biology, chemistry, and physics at PsuKnowHow tutoring center (September 2011- May 2012)

Publication:

Mattie, Floyd J., Melissa M. Rolls, Michelle C. Stone, and Manpreet Parmar. "Directed Microtubule Growth, +TIPs, and Kinesin-2 Are Required for Uniform Microtubule Polarity in Dendrites." *Current Biology*. 20.24 (2010): 1-9.

Language Proficiency:

- English
- Hindi
- Punjabi

References:

Name	Course
Ms. Vickie A. Morgan VMorgan@mountnittany.org	<ul style="list-style-type: none">• Director of Volunteer Services at Mount Nittany Medical Center
Dr. Kimberlyn Nelson kxn4@psu.edu	<ul style="list-style-type: none">• Biol 230M Honors: Molecules & Cells (Fall 2009)
Dr. Stephen W. Schaeffer swschaeffer@psu.edu	<ul style="list-style-type: none">• Biol 110 Honors: Basic Concepts and Biodiversity (Fall 2008)• PSU 016: Biology Freshman Seminar (Fall 2008)
Dr. Melissa Rolls mur22@psu.edu	<ul style="list-style-type: none">• BMB 496 Independent Study/Research (Spring 2009-Fall 2011)